Self-weight effect in the measurement of the volume of silicon spheres

Self-weight effect in the measurement of the volume of silicon spheres

D Mari[1], E Massa[1], N Kuramoto[2] and G Mana[1]

[1]INRIM – Istituto Nazionale di Ricerca Metrologica, str. delle Cacce 91, 10135 Torino, Italy
[2]NMIJ – National Metrology Institute of Japan, National Institute of Advanced Industrial Science and Technology, 1-1-1 Umezono, Tsukuba, Ibaraki 305-8563, Japan

Email: d.mari@inrim.it

Abstract: The volume of ^{28}Si spheres of about 94 mm diameter is an input datum for the determination of the Avogadro constant. We report about a finite element analysis of the self-weight effect on the volume determination via optical interferometric measurements of the sphere diameters. The self-weight expansion or shrinkage of the equatorial diameters, which ranges from −31 pm to +180 pm, depends on the southern latitude of the supports.

Submitted to: *Metrologia*
PACS numbers: 06.20.-f, 06.30.Bp, 02.70.Dh, 06.30.Bp
Keywords: Avogadro constant, volume measurements, kilogram realization, solid density standards, finite element analysis.

1. Introduction

A deep revision of International System of units (SI) is going to be implemented, where fixed conventional values will be given, among others, to the Planck and Avogadro constants [1-3]. Afterwards, the unit of mass, the kilogram, might be realized by counting the atoms in perfect-crystal ^{28}Si spheres of known lattice parameter, volume, surface status (as regards as geometry, physics, and chemistry), isotopic composition, and chemical purity [4-6]. The sphere diameter is about 94 mm, giving a mass close to 1 kg. The artefact calibration will require periodic surface characterizations and volume measurements.

Since the form error, defined as the maximum radial peak-to-valley distance, is less than 100 nm, the volume is determined as $\pi D^3/6$, where D is the mean diameter [7]. Starting from about 10^3 diameter values obtained by repeating optical-interferometric measurements after rotation and repositioning of the sphere on three kinematic supports, NMIJ estimates the mean diameter to within a fractional uncertainty of 6.6 nm/m [5,8]. To support and to complement the measurements, this paper reports on a finite element analysis [9] of the self-weight deformation of the sphere.

2. Measurement of the sphere diameters

The sphere diameters are measured by optical interferometry. At the NMIJ, the sphere is placed in a fused-quartz Fabry–Perot etalon enclosed in a vacuum chamber equipped with an active temperature control. The sphere is supported by three pins placed at 120° azimuthal distance. The interferometer senses the sphere diameter in the horizontal plane, in a fixed direction at 30° azimuthal distance from one of the pins. A two-axis rotation mechanism is placed under the sphere, to repositioning it and to measure the diameters in directions distributed as uniformly as possible. After reorienting the sphere, measurements are repeated to collect and to average more than 10^3 diameter values. The uncertainty of the mean diameter (not corrected for the phase shift due to the surface oxide layer) is 0.62 nm, to which a fractional uncertainty of 6.6 nm/m will correspond [5]. The diameter measurements are made after repositioning the sphere so that, when measured, each diameter locates always in the same direction with respect to the supports. Therefore, the self-weight of the sphere might originate a systematic measurement bias.

3. Finite element analysis

The Young modulus (the stress to strain ratio in the stretching direction, E) and the Poisson ratio (transverse-strain to stretching-strain ratio, ν) of silicon depend on the load direction, that is, on the sphere orientation with respect to gravity. We used the elastic constants given in [10], that is, for the <100> directions, c_{11}

= 165.6 GPa, c_{12} = 63.9 GPa, and c_{44} = 79.5 GPa. The stiffest direction is about [111], where E = 189 GPa; the stretchiest is [100], where E = 130 GPa. The silicon density was set to 2329 kg m^{-3}, the gravity acceleration to 9.807 m s^{-2}.

To make the analysis the simplest, since the expected strain is less than 10 nm/m and we are not interested in the sphere deformation but only in the mean diameter as experimentally determined, we used a linear and isotropic model, where the ν/E ratio, 1.42 x 10^{-3} GPa^{-1}, was set equal to the ratio average over all the crystallographic directions. In practice we set E = 160 GPa and ν = 0.228. Heuristically, we assumed that the mean of the measured diameters of an anisotropic sphere is equal to the diameter measured by using an isotropic sphere whose ν/E ratio is averaged over the crystallographic directions. Moreover, since the diameters are always measured in the same direction with respect the supporting pins, the isotropy assumption avoids a detailed simulation of the measurement procedure, as the result depends only on the measurement direction and not on the orientation of the sphere in the gravitational field. Therefore, only one computation of the elastic deformation is necessary.

As results of a trade-off between processing time and accuracy, about 57000 tetrahedral mesh elements were used. Boundary conditions must be specified to fix the finite element model in space. Since the prescription of Dirichlet boundary conditions on the surface elements (that is, the prescription of fixed translational and rotational degrees of freedom) originates non-physical effects, the sphere supports were included in the analysis. In practice, we united the sphere and supports by generating a composite object consisting of connected domains of different material sharing the boundaries between the neighbours. In this way, the needed Dirichlet boundary conditions were prescribed on the supports' backside-elements.

3.1 Accuracy of the finite element model

The finite element model [9] must not depend on the mesh used. Hence, when the isotropy assumption is made and the constraints are azimuthally invariant, the self-weight deformation must be axially symmetric and must depend only on the polar angle. Therefore, to investigate the numerical accuracy achievable by the finite element model, we carried out studies where – to ensure axial symmetry – the sphere is supported by a steel ring and flared cylinder as shown in Figs. 1 and 2. The material parameters of the support are 7850 kg m^{-3} density, 200 GPa Young's modulus, and 0.30 Poisson's ratio. The deformations of the equatorial diameters were calculated for different azimuths, with steps of 1°; the results are shown in the Figs. 3, 4, 5, and 6, where the diameters are identified by the elevation (latitude) of their northern extremes. As expected, the diameters of the deformed sphere are independent of the azimuthal coordinate. The azimuthal deviations from the mean diameter shown in Figs. 4 and 6 are less than 1 pm. The equatorial diameters deviate from a constant less than 0.1%.

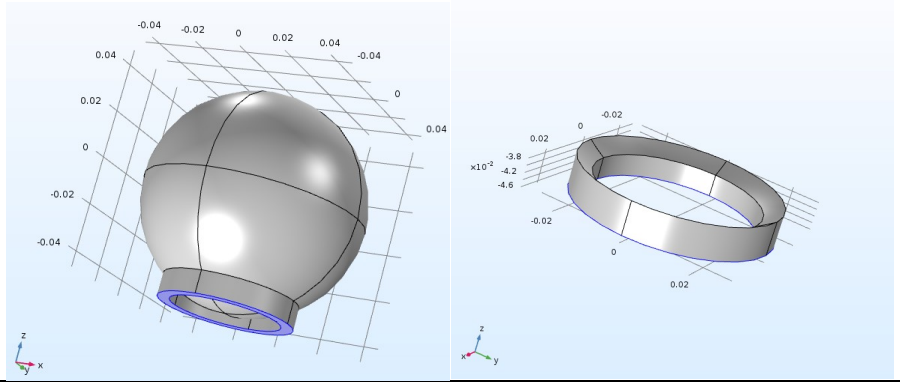

Figure 1. Silicon sphere with a steel ring support. The ring external and internal heights are 9.565 mm and 6.230 mm, the thickness is 5 mm, the external radius is 56.5 mm.

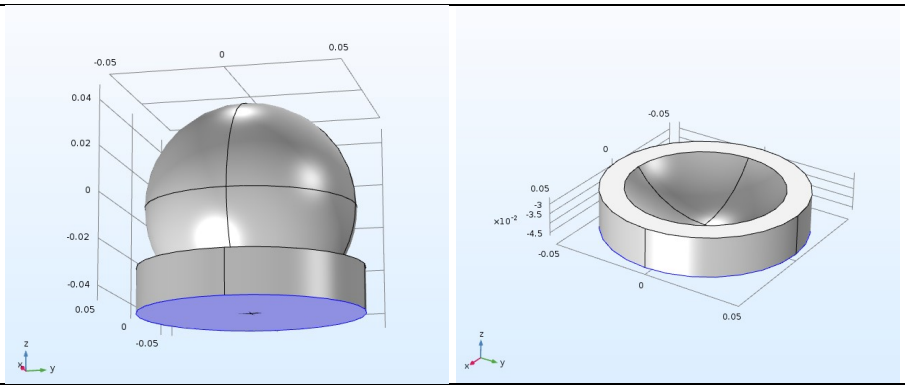

Figure 2. Silicon sphere with a steel flared cylindrical support. The support height is 20 mm, the thickness is 1.79 mm.

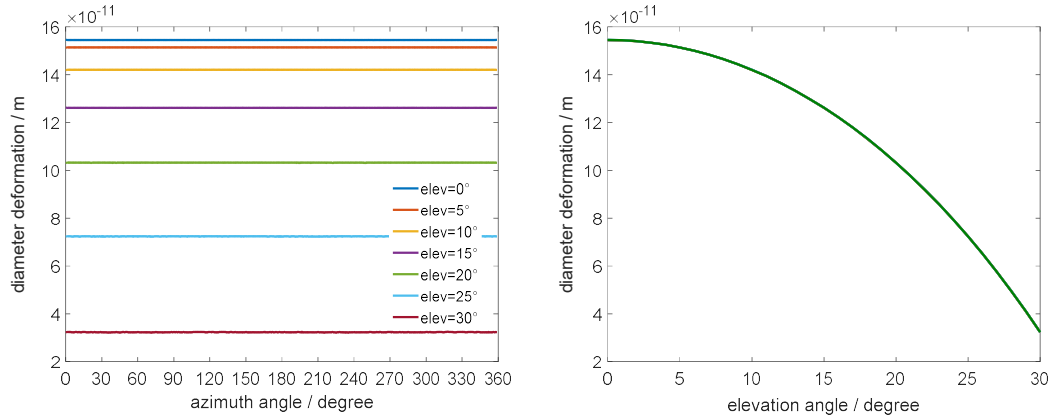

Figure 3. Ring support: Self-weight deformation of the sphere diameters as a function of the azimuth (left) and elevation of the northern extremes (right). Positive deformations indicate larger diameters. The mean deformation of the equatorial diameters is 154.5 pm.

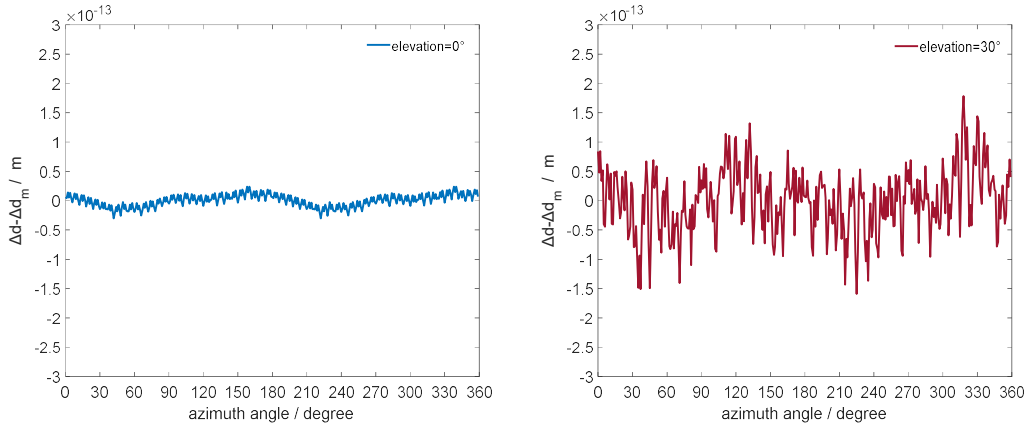

Figure 4. Deviations from the mean diameter deformation, Δd_m, at an elevation of the northern extreme of 0° and 30° (ring support).

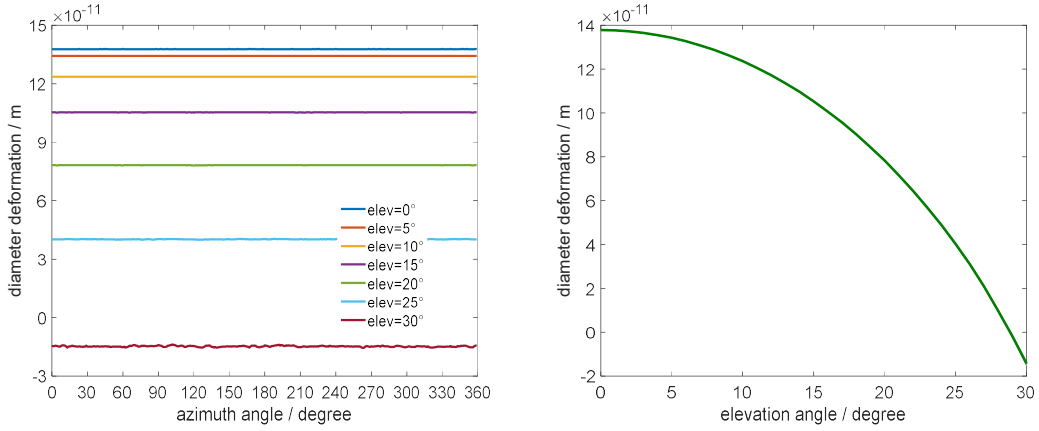

Figure 5. Flared cylindrical support: Self-weight deformation of the sphere diameters as a function of azimuth (left) and elevation of the northern extremes (right). Positive deformations indicate larger diameters. The mean deformation of the equatorial diameters is 137.8 pm.

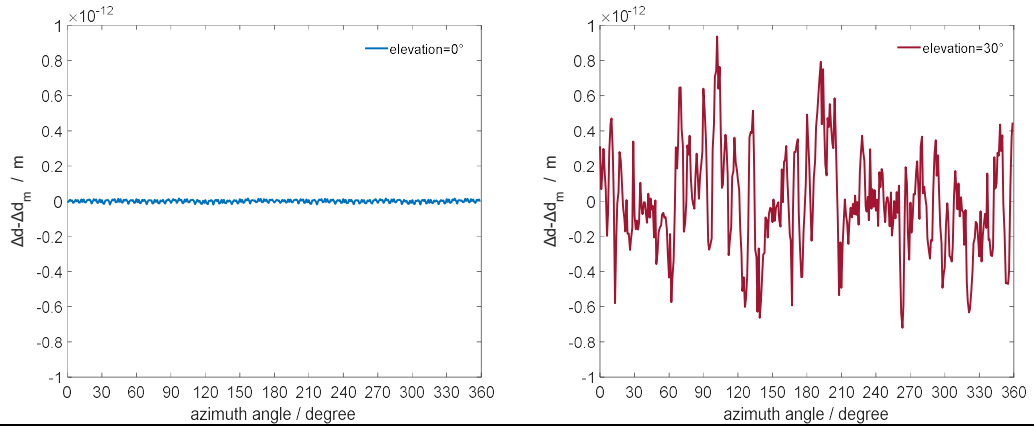

Figure 6. Deviations from the mean diameter deformation, Δd_m, at an elevation of the northern extreme of 0° and 30° (flared cylindrical support).

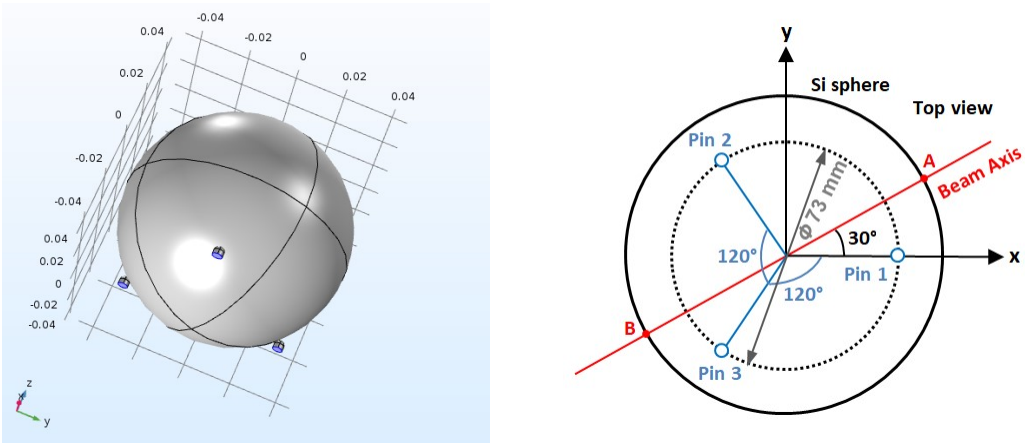

Figure 7. Left: silicon sphere with the supporting pins. Right: top view of the sphere resting on three support at 128.8° polar angle (38.8° south latitude) and spaced by 120° azimuthal angles. The zero meridian goes through the first pin and the azimuths are positive in the counterclockwise direction. The measured diameter AB lies in the equatorial plane at 30° east of the first pin.

1.1 Support modeling

As shown in Fig. 7, the sphere model is supported by three pins, having 4 mm diameter and tip radius equal to 2 mm. The pins are placed at 0°, 120°, and 240° azimuths and 128.8° polar angle (38.8° south latitude) in accordance with the experimental layout adopted by NMIJ [5]. The line AB is the measured (equatorial) diameter at 30° east of the first pin.

As said, we united the sphere and supports into a composite object consisting of connected domains of different material sharing the contact area. To illustrate the impact of the pin material and contact area on the analysis, Fig. 8 shows the deformation of the measured equatorial diameter (at 30° azimuth) sensed the laser beam as a function of the contact area (ranging from 0.0036 mm^2 to 28 mm^2) and material, steel, aluminium, and polyether ether ketone (PEEK). The material properties used are listed in table 1. The maximum deformation difference, between steel and PEEK, is 7 pm. The positive mean-deformation originates from the equatorial bulging of the sphere. As it is shown in Figs. 9 and 10, the indentation of the sphere surface by the supports modulates the deformation of the equatorial diameters with a 60° periodicity. The minima occur at the longitudes of the supports and of their antipodes, the maxima at the indentation ridges. The 30° azimuth of the measured diameter corresponds to a deformation maximum; therefore, the smaller the contact area, the larger the measured diameter.

Table 1. Material properties of the sphere support.

	density / kg m^{-3}	Young's modulus / GPa	Poisson coefficient
steel	7850	200	0.30
Al	2700	70	0.33
PEEK	1320	3.6	0.38

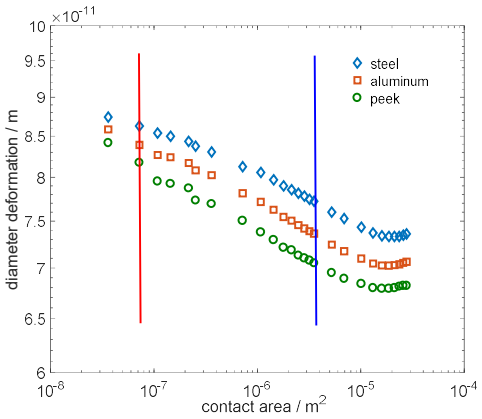

Figure 8. Self-weight deformations of the measured diameter as a function of the contact area between the sphere and the supports. Positive deformations indicate larger diameters.

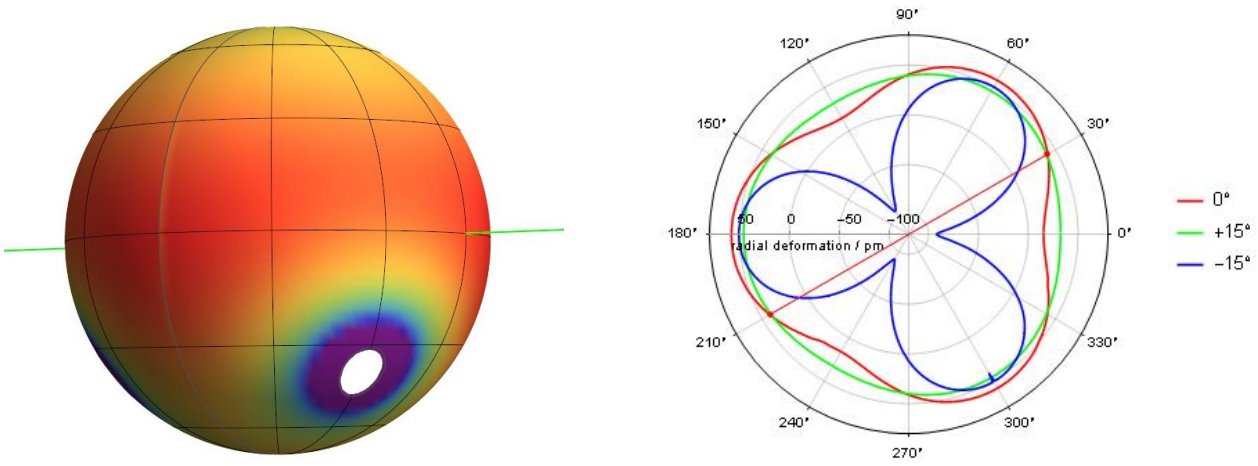

Figure 9. Left: map of the radial deformation of the sphere (0.076 mm^2 contact area). The colour scale is from –300 pm (violet) to 60 pm (red). The contact areas are excluded from the map because of the large deformation, more than 1 nm (saturated area). The green line indicates the laser beam and the measured equatorial diameter at 30° east with respect the first-pin meridian. Right: polar plots of the radial deformation at the equator and ±15° elevations. The red line is the measured diameter.

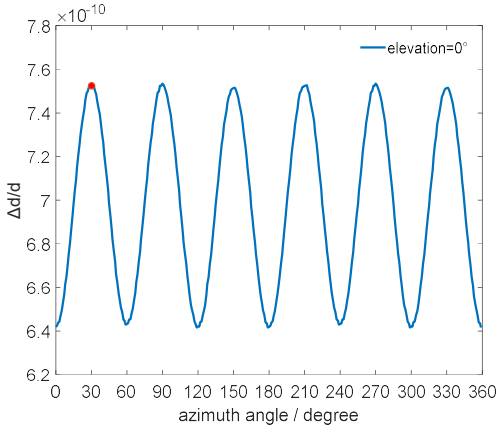

Figure 10. Strains of the equatorial diameters (PEEK supports, 3.5 mm^2 contact area); the red marker indicates the measured diameter. Positive deformations indicate larger diameters.

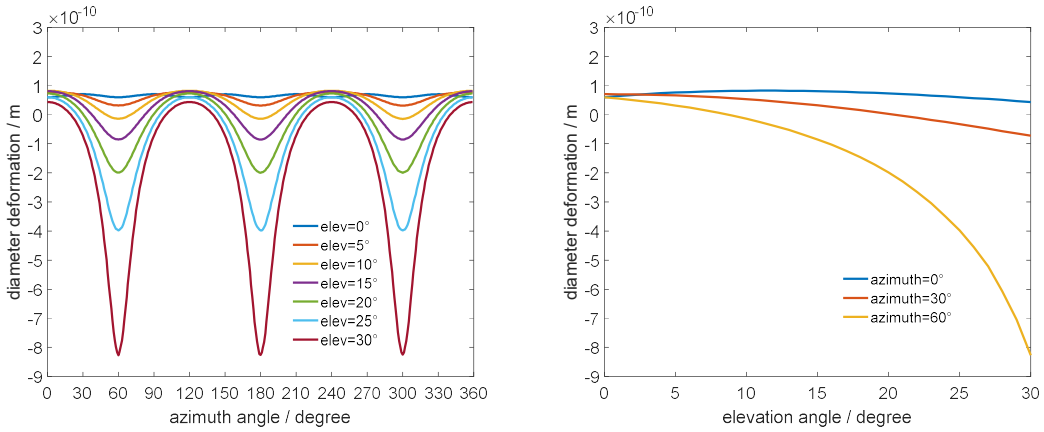

Figure11. Self-weight deformation of the sphere diameter as a function of azimuth (left) and elevation (right, PEEK supports, 3.5 mm^2 contact area). Positive deformations indicate larger diameters.

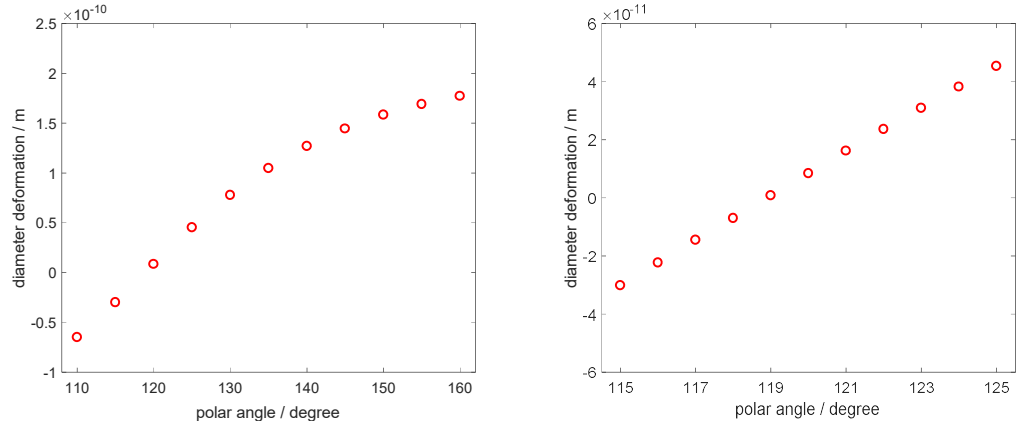

Figure 12. Left: self-weight deformation of the measured diameter (at zero elevation and 30° azimuth) as a function of the polar angle of the PEEK supports (3.5 mm^2 contact area). Right: zoom for polar angles from 115° to 125°. Positive deformations indicate larger diameters.

1.2 Results

In the NMIJ set-up, the pins are made of aluminium and are coated with a PEEK layer. In the case of PEEK supports, the depth of the Hertzian indentation between the Si and PEEK spheres [11], about 4 µm, is less than the coating thickness, which was estimated to be a few tens of micrometres. Therefore, to calculate the deformation of the diameters measured at the NMIJ, we assumed that the supports are entirely made of PEEK and estimated the contact area, about 0.076 mm^2, by using the Hertz theory of spherical indentation. Figure 9 shows the radial deformation of the sphere. The indentations due to the supports, which amount to more than 1 nm, are clearly visible as well as the equatorial ridges midway the indentations. The measured diameter, at 30° east of the first pin, was found to expand by 82 pm, corresponding to a strain of 0.88 nm/m. Therefore, the diameter measured by the interferometer is larger by 82 pm than the diameter of the undeformed sphere.

Figures 10 and 11 show the results of the finite element analysis for PEEK supports and 3.5 mm^2 contact area, where the azimuth and elevation coordinates refer to the northern extreme of the diameter. As expected, a three-fold rotational symmetry substitutes for the axial symmetry around the vertical. The large deformations having 120° periodicity are due to the indentations of the sphere surface by the three supports, whose antipodes' azimuths are 60°, 180°, and 300°. The higher the elevation, the greater the deformation. Besides, at the 38.8° elevation and 60°, 180°, and 300° azimuths, the southern extremes of the diameters will cross the supports.

The equatorial diameters are affected by the smallest deformation, $7\times10^{-10}d$ on the average, having 60° periodicity and $6\times10^{-11}d$ amplitude. The deformation periodicity doubles because now one or the other diameter extremes crosses the indentations.

Figure 12 shows the impact of the polar angle of the PEEK supports on the measured equatorial diameter at 30° azimuth, calculated in the case of a 3.5 mm^2 contact area. There exists an optimal support location, at about 119° polar angle, ensuring that the strain of the measured diameter is null.

3. Conclusions

We studied, by finite element analysis, the impact of gravity on NMIJ's volume-determination of a silicon sphere, where, after repositioning of the sphere, the measured diameter is always in the equatorial plane, at the same azimuthal distance from three kinematical supports. To make the analysis the simplest, we used a linear and isotropic model, where the ν/E ratio was equal to its average over the crystallographic directions.

Firstly, we investigated the numerical accuracy of the finite element model by studying axisymmetric geometries, where the sphere strain must not depend on the azimuthal angle. The calculation of the equatorial strain was validated to within a numerical accuracy better than 1%. The accuracy of the final model has been confirmed by observing a strain field having the same three-fold rotational symmetry of the supports and boundary conditions. Secondly, we assessed the modelling of the sphere supports, as regards as material and contact area, and the effect of the boundary conditions.

In the case of the NMIJ measurement geometry, with PEEK-coated aluminium supports – placed at 38.8° south latitude and having a 0.076 mm^2 contact area – and the isotropy approximation, we estimated a systematic expansion of the measured diameter equal to 82 pm, corresponding to a fractional error of 0.88 nm/m. This corresponds to a fractional overestimation of the sphere volume equal to 2.6×10^{-9}, to be compared with a fractional uncertainty of the apparent volume measurement (not corrected for the phase shift due to the surface oxide layer) equal to 20×10^{-9} [5]. The effect of the self-weight deformation on the volume determination is therefore negligibly small. Eventually, it was found that an optimal location of the sphere support exists, which nullifies this error.

Recent results reported by the Physikalische Technische Bundesanstalt (PTB) have shown that achieving a fractional uncertainty of the apparent sphere volume as small as 4.5×10^{-9} is possible [12] and that the sphere topography can be optically reconstructed to within a few tens of picometers sensitivity [13]. Therefore, future works will extend the analysis to take the crystal asymmetry into account and investigate the feasibility of experimental tests of the finite element model.

Acknowledgments

This analysis was based on the investigations of M Tanaka (retired from the NMIJ) and G Bertolotto Blanc (now at ABB Italy) who anticipated and laid the foundations of this study twenty years ago at the then National Research Laboratory of Metrology of Japan. This work was supported in part by the Grant-in-Aid for Scientific Research (B) (KAKENHI 16H03901) from the Japan Society for the Promotion of Science.

References

[1] Bettin H and Schlamminger S 2016 Realization, maintenance and dissemination of the kilogram in the revised SI *Metrologia* **53** A1-A5

[2] Robinson I A and Schlamminger S 2016 The Watt or Kibble balance: a technique for implementing the new SI definition of the unit of mass *Metrologia* **53** A46-A74

[3] Fujii K *et al*., 2016 Realization of the kilogram by the XRCD method *Metrologia* **53** A19-A45

[4] Azuma Y *et al.* 2015 Improved measurement results for the Avogadro constant using a ^{28}Si-enriched crystal *Metrologia* **52** 360-375

[5] Kuramoto N *et al.* 2017 Determination of the Avogadro constant by the XRCD method using a ^{28}Si-enriched sphere *Metrologia* **54** 716-729

[6] Bartl G *et al.* 2017 A new ^{28}Si single crystal: counting the atoms for the new kilogram definition, *Metrologia* **54** 693-715.

[7] Mana G 1994 Volume of quasi-spherical solid density standards *Metrologia* **31** 289-300

[8] Kuramoto N, Fujii K and Yamazwa K 2011 Volume measurements of ^{28}Si spheres using an interferometer with a flat etalon to determine the Avogadro constant *Metrologia* **48** S83-S95

[9] COMSOL Multiphysics® 5.2a

[10] Hopcroft M A 2010 What is the Young's Modulus of Silicon*? J. Microelectromech. Syst.* **19** 229-238

[11] Johnson K L 1987 *Contact Mechanics* Cambridge University Press

[12] Nicolaus A, Bartl G, Peter A, Kuhn E and Mai T 2017 Volume determination of two spheres of the new ^{28}Si crystal of PTB *Metrologia* **54** 512-515

[13] Mai T and Nicolaus A 2017 Optical simulation of the new PTB sphere Interferometer *Metrologia* **54** 487-493